

A radiometric analysis of projected sinusoidal illumination for opaque surfaces

Michael Holroyd
University of Virginia

Jason Lawrence
University of Virginia

Todd Zickler
Harvard University

Abstract

Shifted sinusoidal illumination patterns are useful for appearance capture because they simultaneously separate local and non-local reflections and allow the recovery of surface geometry. Here we show that the same illumination patterns can be used to estimate the local surface reflectance (BRDF) as well, provided that an appropriate correction factor is applied. We derive a closed-form expression for this correction factor, validate it experimentally, and discuss its implications.

1 Preliminaries

Consider the system in Fig. 1. A thin-lens camera observes a planar surface patch that is illuminated by a custom light assembly, and this light assembly consists of a planar Lambertian area source placed at the focal plane of another thin lens. The area source in this light assembly produces radiance patterns that are shifted horizontal sinusoids with fixed frequency f , amplitude A , and DC offset G . The shifts are represented by a discrete set of phase values: $\{\phi_k\}_{k=1\dots M}$, so we can write the radiance at a point $\mathbf{p} = (p, q)$ on the focal plane of the source as

$$L^k(p, q) = A \cos(2\pi f(p + \phi_k)) + G, \quad k = 1 \dots M. \quad (1)$$

Illumination from the source is focused at a point \mathbf{x} on a planar surface patch, and this patch is observed by a thin-lens camera, which is also focused at \mathbf{x} . A pixel (or any square region) on the image plane that is centered at the projection of \mathbf{x} and has dimensions $w \times w$ measures flux due to the radiance from a neighborhood of the point \mathbf{x} on the surface, and assuming that the camera is a linear device, the intensity recorded at the pixel is proportional to this flux. Under the sinusoidal illumination of Eq. 1, the pixel response can be written in the form,

$$I^k(\mathbf{u}) = \alpha(\mathbf{u}) \cos(\gamma t_k + \phi(\mathbf{u})) + \beta(\mathbf{u}), \quad k = 1 \dots M, \quad (2)$$

where $\mathbf{u} = \Pi_c(\mathbf{x})$ is the projection of \mathbf{x} (the center of the pixel), and $\gamma = 2\pi f(t_{k+1} - t_k)$, the product of the spatial frequency and the displacement of the sinusoid between consecutive shifts. This relation plays a central role in phase mapping techniques (e.g. [4]), since the *apparent phase* $\phi(\mathbf{u})$ provides information about the depth of the surface along the ray that is back-projected from pixel \mathbf{u} .

Presently, we are interested in the *apparent amplitude* $\alpha(\mathbf{u})$ since, as we will show, it provides information about the local surface reflectance (the BRDF at \mathbf{x}) and can be used for reflectometry. We show that, in addition to the BRDF, this expression depends on the intrinsic parameters of the lightsource and camera, as well as their positions and orientations relative to the surface.

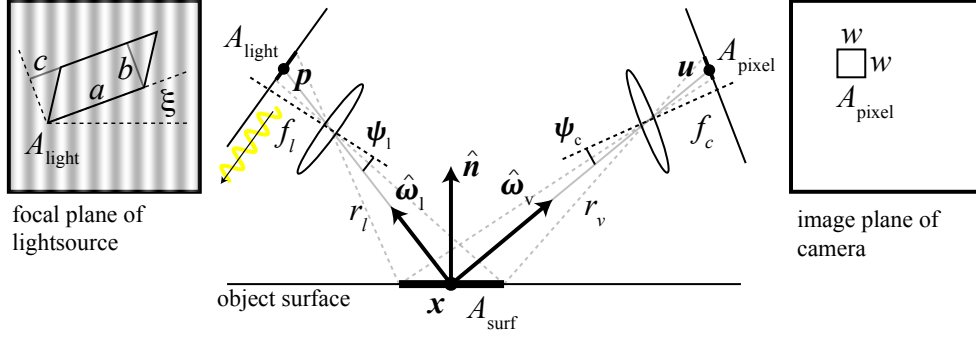


Figure 1: A square pixel in the camera projects, via a planar surface patch, to an oriented parallelogram in the focal plane of a focused light source. We are interested in the relationship between the amplitude of the translating sinusoidal radiance pattern on the focal plane of the light source and the apparent amplitude at the camera’s pixel. Note that the regions A_{light} and A_{pixel} are not drawn to scale.

2 Relating projected and observed sinusoids

We obtain flux incident on the image plane from radiance emitted from the focal plane of the source using three basic relations.

Image irradiance from surface radiance. The image irradiance $E_c(\mathbf{u})$ that is due to radiance $L_s(\mathbf{x}, \hat{\omega}_v)$ at surface point \mathbf{x} in direction $\hat{\omega}_v$ is given by the familiar thin-lens equation (e.g. [1]),

$$E_c(\mathbf{u}) = \sigma(\mathbf{u})L_s(\mathbf{x}, \hat{\omega}_v). \quad (3)$$

Here, $\sigma(\mathbf{u})$ models optical fall-off in the camera, which for a thin lens depends on the area of the camera’s aperture, its focal length, and the angle ψ_c between its optical axis and the ray through \mathbf{u} : $\sigma(\mathbf{u}) = \sigma(\psi_c) = A_c \cos^4(\psi_c)/f_c^2$. (See Fig. 1 and Table 1 for summaries of notation.) More generally, this sensitivity function can be measured during a radiometric calibration procedure, and we assume it to be known.

Emitted radiance from incident irradiance at the surface. This relation simply follows from the definition of the bi-directional reflectance distribution function, or BRDF [3]:

$$L_s(\mathbf{x}, \hat{\omega}_v) = \rho(\hat{\omega}_i, \hat{\omega}_v)E_s(\mathbf{x}). \quad (4)$$

We assume that the scattering properties are statistically uniform over the small area A_{surf} observed by a single pixel, and that following the isolation of local reflections [2], light transport within the material occurs over distances that are small relative to this area.

Surface irradiance from radiance on the source focal plane. This relation is less familiar, so we provide a derivation. The basic idea is to compute the power emitted from the focal plane of the source toward its lens, and then divide this by the differential surface area δS to obtain surface irradiance. The underlying assumption is that δS is in focus, so that all of the power that reaches the lens arrives at δS .

Let L be the emitted radiance at the center of a differential patch $\delta \mathbf{p}$ on the focal plane of the source assembly. The power received by the lens is this radiance multiplied by the differential area foreshortened in the direction of travel and the solid angle subtended by the lens as seen by this small area:

$$\Phi = L\delta \mathbf{p} \cdot \cos \psi_1 \cdot \frac{A_l \cos \psi_1}{(f_l^2 / \cos^2 \psi_1)} = L\delta \mathbf{p} \cdot \frac{A_l \cos^4 \psi_1}{f_l^2}.$$

Table 1: Summary of notation

\mathbf{x}	scene point
$\mathbf{u} = (u, v)$	point on image plane of camera
$\mathbf{p} = (p, q)$	point on focal plane of lightsource
$d\mathbf{u}, d\mathbf{p}, dS$	differential areas on the image plane, source plane, and surface
$\hat{\mathbf{n}}$	surface normal
$\hat{\omega}_l, \hat{\omega}_v$	local light and view directions
$\rho(\hat{\omega}_l, \hat{\omega}_v)$	BRDF
$\sigma(\mathbf{u})$	camera sensitivity function
$l(\mathbf{x})$	lightsource emission function
f_l, f_c	focal lengths of lightsource and camera
ψ_l, ψ_c	angles from optical axes of lightsource and camera
r_l, r_c	distances from scene point to lightsource and camera centers
$A_{\text{pixel}} = w^2$	area of square camera pixel
A_{surf}	area of corresponding region on surface
$A_{\text{light}} = ab$	area of corresponding parallelogram on source focal plane
c	signed distance that characterizes the degree of skew in parallelogram
A_l, A_c	areas of lightsource and camera apertures
Ω_l, Ω_c	solid angles subtended by lightsource and camera as seen by surface
$E_s(\cdot), E_c(\cdot)$	irradiance at the surface, and image plane of camera
$L(\cdot), L_s(\cdot)$	radiance emitted at the lightsource, and surface
$\Phi(\cdot)$	power (flux)

Since it is in focus, all of this power arrives at a differential area on the surface δS , and the surface irradiance is $E_s = \Phi/\delta S$. The ratio of areas can be obtained by equating the solid angles subtended by $\delta \mathbf{p}$ and δS as seen by the center of the lens,

$$\frac{\delta \mathbf{p}}{\delta S} = \frac{f_l^2}{r_l^2} \frac{(\hat{\mathbf{n}} \cdot \hat{\omega}_l)}{\cos^3 \psi_l}, \quad (5)$$

and combining these expressions yields the desired relationship:

$$E_s = A_l \cos \psi_l \cdot L \cdot \frac{(\hat{\mathbf{n}} \cdot \hat{\omega}_l)}{r_l^2}.$$

Analogous to the camera sensitivity function described above, in practice we generalize this expression to

$$E_s = l(\mathbf{x})L(\hat{\mathbf{n}} \cdot \hat{\omega}_l), \quad (6)$$

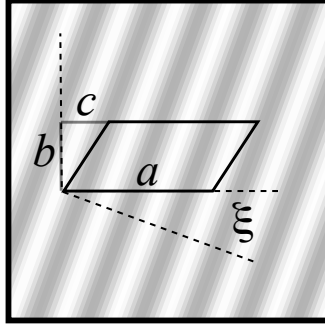
where $l(\mathbf{x})$ is an *emission function* that can be measured during a radiometric calibration process and is assumed to be known.¹

Equipped with Eqs. 3, 4, and 6, we are ready to proceed. The power received by the finite pixel area A_{pixel} centered at image point \mathbf{u}_o (and thus the response of that pixel) is the integral of the image irradiance, which by Eq. 3 is

$$\Phi_{\text{pixel}} = \sigma(\mathbf{u}_o) \int_{A_{\text{pixel}}} L_s(\Pi_c^{-1}(\mathbf{u})) d\mathbf{u},$$

where $\Pi_c^{-1}(\cdot)$ is the back-projection of image point \mathbf{u} onto the surface. (In this expression, we have assumed the sensitivity function to be constant over the pixel.) Using an expression analogous to Eq. 5, we change

¹In fact, as described in the main paper, we find it beneficial to incorporate the r_l^2 term into this function and thus allow it to vary over the three-dimensional working volume: $l(\mathbf{x})$.



focal plane of lightsource

Figure 2: The source region A_{light} corresponding to a single camera pixel, depicted in a transformed coordinate system (p', q') that aligns one side of the region with a coordinate axis (compare to the left of Fig. 1). The shape of this parallelogram is determined by the lengths of its sides, a and b , and its skew, which is characterized by the *signed* distance c . These parameters, along with the position and orientation ξ relative to the horizontal axis of the source focal plane can be computed from the known surface geometry and the parameters of the lightsource and camera.

variables to integrate over the observed area (A_{surf}) on the surface instead, and this yields

$$\Phi_{\text{pixel}} = \sigma(\mathbf{u}_o) \frac{f_c^2}{\cos^3 \psi_c} \frac{(\hat{\mathbf{n}} \cdot \hat{\boldsymbol{\omega}}_v)}{r_c^2} \int_{A_{\text{surf}}} L_s(\mathbf{x}) dS,$$

when the pixel is small enough for the angles and distances $(\psi_c, r_c^2, \hat{\boldsymbol{\omega}}_v)$ to be constant over its extent.

Finally, the surface radiance is related to the radiance on the source focal plane through Eqs. 4 and 6, and making these substitutions along with another change of variables, $dS \rightarrow d\mathbf{p}$, gives

$$\Phi_{\text{pixel}}^k = \sigma(\mathbf{u}_o) l(\mathbf{p}_o) \frac{f_c^2 \cos^3 \psi_1}{f_l^2 \cos^3 \psi_c} \frac{(\hat{\mathbf{n}} \cdot \hat{\boldsymbol{\omega}}_v)}{r_c^2} \rho(\hat{\boldsymbol{\omega}}_1, \hat{\boldsymbol{\omega}}_v) \int_{A_{\text{light}}} L^k(\mathbf{p}) d\mathbf{p}. \quad (7)$$

The last term in this expression is the integral of the sinusoidal radiance pattern (Eq. 1) over an area A_{light} that is obtained by projecting the square pixel A_{pixel} onto the planar surface and into the lightsource. The area A_{light} is a quadrilateral that, due to the small extent of a single pixel, is relatively unaffected by perspective distortion and is well-approximated by a parallelogram, as depicted in Fig. 1 and Fig. 2. Any such parallelogram is completely described by the lengths of its sides, a and b , its orientation ξ relative to the horizontal axis of the source focal plane, the position $\mathbf{p}_o = (p_o, q_o)$ of its center, and its skew, which we parameterize by the *signed* distance c shown in Fig. 2. In the present case, all of these parameters are determined by the camera and source parameters and the surface position and orientation, and since all of these are known, we can compute the parallelogram parameters corresponding to any pixel in our camera.

In order to compute the integral over this region, we first change the coordinate system to be aligned with side b and have one corner as its origin as shown in Fig. 2. We use (p', q') for these new coordinates, which allow us to write the integral as

$$\int_{A_{\text{light}}} L^k(\mathbf{p}) d\mathbf{p} = \int_0^b \int_{\frac{c}{b}p}^{\frac{c}{b}p+a} G + A \cos(2\pi f(p' \cos \xi - q' \sin \xi + p_o + \phi_k)) dp' dq'.$$

By twice using the identity $\int \cos(sx + t)dx = \sin(sx + t)/s$, performing trigonometric manipulations, and using the expression $\text{sinc}(x) = \sin(\pi x)/(\pi x)$, we obtain

$$\int_{A_{\text{light}}} L^k(\mathbf{p})d\mathbf{p} = ab(A \text{sinc}(af \cos \xi) \text{sinc}(bf \sin \xi + cf \cos \xi) \cos(\pi f(b \sin \xi + a \cos \xi + c \cos \xi + p_o + \phi_k)) + G).$$

Now, substituting this into Eq. 7, we obtain an expression for the flux Φ_{pixel}^k (and thus the pixel response) that is in the desired form of Eq. 2. From this it follows that the apparent amplitude of the observed sinusoid in the camera satisfies

$$\alpha(\mathbf{u}_o) \propto \sigma(\mathbf{u}_o)l(\mathbf{x})\rho(\hat{\omega}_1, \hat{\omega}_v)(\hat{\mathbf{n}} \cdot \hat{\omega}_1)A \text{sinc}(af \cos \xi) \text{sinc}(bf \sin \xi + cf \cos \xi), \quad (8)$$

where we have used the fact that the total area of the parallelogram $A_{\text{light}} = ab$ is given by

$$ab = w^2 \frac{(\hat{\mathbf{n}} \cdot \hat{\omega}_1)r_c^2 f_l^2 \cos^3 \psi_c}{(\hat{\mathbf{n}} \cdot \hat{\omega}_v)r_l^2 f_c^2 \cos^3 \psi_l}.$$

3 Implications for reflectometry: “amplitude loss”

The result in Eq. 8 confirms that the apparent amplitude measured at each camera pixel $\alpha(\mathbf{u})$ (Section 5.2 in the main paper) is proportional to the product of the surface irradiance under point lighting $l(\mathbf{x})(\hat{\mathbf{n}} \cdot \hat{\omega}_1)$ (recall that $1/r_l^2$ is captured by $l(\mathbf{x})$), the amplitude of the projected sinusoidal illumination A , the BRDF $\rho(\hat{\omega}_1, \hat{\omega}_v)$, and the camera sensitivity $\sigma(\mathbf{u})$. In addition, it also predicts a less obvious effect that we call “amplitude loss” whereby the measured response is inversely proportional (via the sinc functions) to the product of the pixel width w and the frequency f of the source radiance pattern in addition to the relative orientations and distances between \mathbf{x} and the camera and source. In words, if either f or w increase (holding everything else fixed) the measured amplitude will decrease at a rate predicted by the product of the sinc functions in Equation 8 and eventually reach zero — this corresponds to the point at which the sine pattern is no longer visible in the image. Similarly, as the camera approaches a grazing view of the surface in a direction perpendicular to that of the sine wave with an overhead source held fixed or the distance from \mathbf{x} to the camera r_v increases, then the measured amplitude will similarly decrease. This makes Eq. 8 a useful analytic tool for estimating the lower bounds on f for a particular experimental setup and, more importantly, it allows converting the amplitude measured at the camera into measurements of the surface BRDF.

The graphs in Fig. 3 confirm this effect and validate the analytic model derived above. They show the amplitude measured at a camera pixel as it moves toward the horizon $(\hat{\mathbf{n}} \cdot \hat{\omega}_v) \rightarrow 0$ with its up vector in the epipolar plane and for a stationary overhead light $(\hat{\mathbf{n}} \cdot \hat{\omega}_1) = 1$. For this “in-plane” configuration, the parallelogram reduces to a rectangle ($c = 0$). The three graphs correspond to different orientations of the sine wave with respect to the plane of motion. These graphs also include predictions by a numerical simulation that agree with our analytic model exactly — we have verified that this is true beyond the in-plane case illustrated here. Note that this amplitude loss can be significant. In the case where $\xi = 0$, a roughly 20% decrease in the amplitude is observed at an elevation angle of 60 degrees which falls off to roughly 90% at 80 degrees.

In practice, when using measured amplitudes $\alpha(\mathbf{u})$ for reflectometry, we correct for this effect by dividing by the terms on the right-hand side in Eq. 8 in order to isolate the BRDF $\rho(\hat{\omega}_1, \hat{\omega}_v)$.

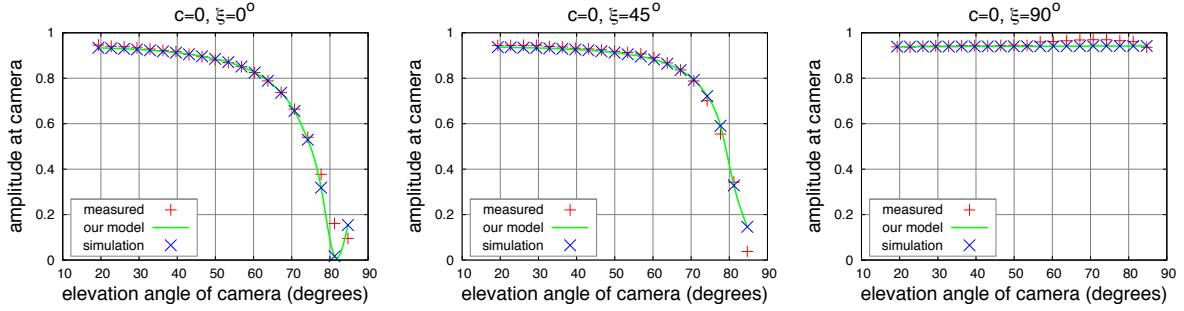


Figure 3: Measurements and simulation results confirming the “amplitude loss” phenomenon and validating our analytic model. Each graph shows the amplitude measured at a single camera pixel as the view direction approaches the horizon ($\hat{n} \cdot \hat{\omega}_v \rightarrow 0$) with the light source held fixed overhead ($\hat{n} \cdot \hat{\omega}_1 = 1$). The camera’s up vector remains in the epipolar plane, causing the parallelogram A_{light} to reduce to a rectangle ($c = 0$). For the measurements, we imaged a Spectralon board and corrected for deviations from a perfect Lambertian reflector. We used the parameters of our experimental setup (focal lengths, pixel size, stand-off distances, etc.) to perform a numerical simulation of the amplitude measured at the camera and to evaluate our model in Eq. 8. We observed very close agreement between measured data, our simulation, and our model.

References

- [1] B.K.P. Horn. *Robot vision*. MIT Press Cambridge, MA, USA, 1986.
- [2] Shree K. Nayar, Gurunandan Krishnan, Michael D. Grossberg, and Ramesh Raskar. Fast separation of direct and global components of a scene using high frequency illumination. *ACM Transactions on Graphics (Proc. SIGGRAPH)*, 25(3):935–944, 2006.
- [3] FE Nicodemus, JC Richmond, JJ Hsia, IW Ginsberg, and T. Limperis. Geometrical considerations and nomenclature for reflectance. *National Bureau of Standards Monograph 160*, 1977.
- [4] V. Srinivasan, H. C. Liu, and M. Halioua. Automated phase-measuring profilometry: A phase mapping approach. *Applied Optics*, 24:185–188, 1985.